

Optical tweezers in complex samples

Neus Allande Calvet

Facultat de Física, Universitat de Barcelona, Diagonal 645, 08028 Barcelona, Spain.

Advisors: Estela Martín Badosa, Mario Montes Usategui

The increasing interest in using optical tweezers to study biological samples reveals a need to experiment with irregular objects, since some bacteria and cellular organisms have ellipsoidal or cylindrical shapes. The aim of this project is to study how non-spherical particles respond to optical trapping, specifically using two traps to hold them, instead of one. A Matlab simulation is first performed in order to foresee the behavior of the trapped particle and the force exerted on it, and compare these results with the subsequently data obtained in the Optical Trapping Laboratory.

I. INTRODUCTION

Optical tweezers were developed by Ashkin and co-workers, who in 1986 created the first stable three dimensional trap with a single focused laser beam [1]. This technique was quickly implemented in many laboratories and only a few years later a wide range of applications emerged, starting from the physical sciences as trapping neutral cooled atoms, to the experimentation of biological samples, like studying the DNA mechanical properties, measure the forces exerted by molecular motors and more recently, performing cell nanosurgery [2].

All this has been possible because optical trapping allows to manipulate microscopic samples with a focused laser beam, thanks to the radiation pressure that light exerts on material particles. The light-matter interaction is originated by the change in the light's momentum when it is scattered by an object that, in order to be trapped, must have a refractive index larger than the one of the surrounding medium. The momentum change results in a net force on the object, which is usually splitted in two perpendicular components:

1. **The scattering force:** Pushes the particle in the direction of propagation of the beam in proportion to its intensity, resulting in a net force in the forward direction.
2. **The gradient force:** Pulls the particle towards the laser focus where the light intensity is the highest. Therefore, the object experiences a force in the direction of the electrical field gradient[3].

Regarding this, it is easy to imagine that effective and stable trapping occurs when gradient forces are higher than scattering forces, situation where the object remains stably trapped at the point of highest intensity in the light beam (that typically has a Gaussian intensity profile). This point is at the plane of the beam waist ω_0 where a very steep intensity gradient is achieved by sharply focusing the light beam, using a high NA (numerical aperture) microscope objective immersed in oil or water.

The force exerted by the optical trap is in the order of 0.1 and 100 pN and its magnitude depends on the relative position between the particle and the trap. The

tightly focused beam creates a parabolic potential well for the trapped sample within a region of some hundreds of nanometers [2]. This implies that for small displacements of the particle, the force is proportional to the transverse position of the object from the equilibrium spot, and therefore the optical trap behaves harmonically, acting as a spring and obeying the Hooke's law:

$$F(x) = -kx \quad (1)$$

Where k is the stiffness of the trap and x is the cross-sectional component of the position (perpendicular to the propagation direction of the beam). This harmonic behavior offers the possibility to, once determined the k parameter, use the optical tweezers as a dynamometer to compute the forces exerted on the trapped objects, from the measured position of the sample [4]. However, there are several magnitudes that influence the value of the stiffness such as temperature, the radius of the particle, the ratio between the refractive indexes of the medium and the sample, the numerical aperture of the microscope objective or the laser power [2].

This complicates the measurements because, in order to compute the stiffness, a trap calibration is required for every sample and every time we change any of the named conditions. This traditional approach also relies on the approximation of spherical particles and a region of linear behavior (1), and is only valid if the object is hold with one trap. For this reason, not much research has been devoted to trapping of non-spherical samples, situation where the force profiles are unknown a priori and an assumption of linear behaviour cannot be inferred.

Luckily, there is an advantageous method [5] that can be used to calculate the force directly, with no need to calibrate the stiffness, even if the particles are not spherical [6]. The technique used in our lab experiments consists on directly measuring the momentum change of the trapping beam, collecting the emerging light from the trap at the back focal plane of a condenser lens with a position sensitive detector (PSD) [4]. In order to capture all the light from the trap propagating in the forward direction (that generally represents a 97-99% of the whole power), the numerical aperture of the condenser lens must be larger than the refractive index of the suspension fluid, and the trapped particle must be close to

the upper surface of the sample's chamber, avoiding loss of light. Thus, the signal detected in the PSD is proportional to the force and the conversion factor is constant regardless of the properties of the sample [4]. This approach is very suitable for our intended purpose, as force profiles for the set of two traps on an elongated object must be evaluated.

II. RAY OPTICS SIMULATION

In general, and specially when the size of the particle r is comparable to the wavelength of the trapping light beam λ , the full theory of optical tweezers is quite complex [7] and complete electromagnetic theories are required to supply an accurate description [3]. However, if these magnitudes are significantly different, the mathematical treatment can be simplified using one of the following approaches:

1. **Rayleigh regime** if $r \ll \lambda$. Describes the particle-light interactions using wave optics. The trapped object can be viewed as an induced dipole that feels a Lorentz force due to the gradient in the electric field.
2. **Mie regime** if $r \geq 5\lambda$. Optical forces can be computed from simple ray optics.

Due to the size of the objects involved in our case, as in biological studies, we are interested on using the Mie regime, which offers a very good approximation via geometrical optics bringing an easy approach and reliable results when computing optical forces [2].

In this project, a Matlab software package named **OTGO** (Optical Tweezers in Geometrical Optics [8][9]) is used to obtain theoretical results. Whereas the core code did not need any change, several modifications were made to compute and plot the forces exerted by not one, but two tweezers on a cylinder much larger than the wavelength of the laser beam. Let us explain briefly how this simulations work and how the forces are calculated:

As we mentioned before, when a ray meets a surface between two media of different refractive indexes, there is a change in the direction of the momentum of light p , which originates a force F on it:

$$\frac{d\vec{p}}{dt} = \vec{F} \quad (2)$$

We want to relate this force to the power P of the incident ray, which is conserved, i.e. must be equal to the sum of the power of the transmitted and the reflected ray [8]:

$$P_i = P_r + P_t \quad (3)$$

In general, the power can be expressed as:

$$P = \vec{v} \cdot \vec{F} \quad (4)$$

Where \vec{v} is the velocity of the light ray in each media, described by the ratio between the speed of light in the vacuum c and the refractive index of each medium n . Therefore equation (4) can be written as:

$$P = \frac{cF}{n} \quad (5)$$

And the total optical force done by the incident ray \vec{F}_{ray} , deriving from equations (3) and (5) is a balance of the optical forces in each (unitary) direction: the incoming \hat{u}_i , the reflected \hat{u}_r and the transmitted one \hat{u}_t :

$$\vec{F}_{ray} = \frac{n_m P_i}{c} \hat{u}_i - \frac{n_m P_r}{c} \hat{u}_r - \sum_{j=2}^{\infty} \frac{n_m P_t^{(j)}}{c} \hat{u}_t^{(j)} \quad (6)$$

Where n_m is the refractive index of the surrounding medium. The first summand is the force done by the incoming ray, the second one is the force by the first reflected ray and the third one is the sum of every force exerted by the transmitted ray in each scattering event. Only the first reflection is calculated because most power goes into the transmitted ray, which is computed by the simulation until its power is less than 10^{-12} times the power of the incoming ray, and for a maximum of six scattering events [9]. As all these forces are in a plane, they can be expressed by the scattering and gradient components, as seen in *figure 1*.

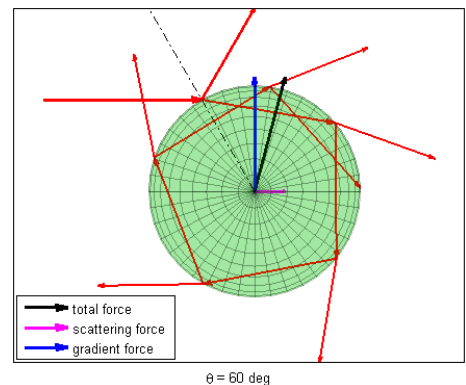


Figure 1: OTGO figure of incident, reflected and transmitted rays (in red) on a sphere, the total force and the gradient and scattering force components, for an incidence angle of 60 degrees.

A Gaussian beam is commonly used on optical trapping experiments [2][3][7] and can be approximated by a bundle of rays parallel to the optical axis, each endowed with a power proportional to the local intensity of the beam [8]. Hence, the total force exerted by the focused beam (i.e. the trap) is then the sum of all rays:

$$\vec{F}_{beam} = \sum_k \vec{F}_{ray}^{(k)} \quad (7)$$

If the object to be trapped is not spherical but elongated, as a cylinder or an ellipsoid, an optical torque also arises, which tends to align the particle with its longest

axis along the longitudinal direction, as can be seen in *figure 2*. This is the main reason why we are interested in using two traps lengthwise to hold one sample, so it can be disposed in the most appropriate way for the experiment.

III. EXPERIMENTAL PROCEDURE

A. Experimental setup

An array of optical tweezers were created with a laser (IPG YLM-5-1064-LP) emitting a continuous beam at an infrared wavelength ($\lambda = 1064$ nm), and controlled with a spatial light modulator (Hamamatsu X10468-03). The laser light enters into a modified inverted microscope (Nikon Eclipse TE2000-U) where, in order to build the trap on the plane of the sample, it is focused with a water-immersion microscope objective (Nikon Plan Apo, 60x, 1.2 NA). The sample illumination and force detection instrument (Impetux Optics, LUNAM T-40i) was disposed in oil-immersion contact with the coverslip of the microscope slide, which contained the sample made of micro-sized silica cylinders of $n_m = 1.55$ suspended in water. This sample was placed above a piezoelectric stage (Piezosystem Jena, TRITOR 102 SG) as seen in *figure 3*, in order to transfer an oscillating movement. Videos and images were registered with a CCD camera connected at one of the ports of the microscope [6].

B. Data acquisition

A known viscous force was applied on the trapped particle to counteract the optical force exerted by the set of traps, so it could be measured. The drag force is originated with a piezoelectric stage (*figure 3*) that, receiving a triangular signal along the transverse direction of the beam, transfers an oscillating movement to the sample, which contains the particles to be trapped suspended in water.

$$\vec{F}_{drag} = \gamma \vec{v} \quad (8)$$

Therefore, the drag force \vec{F}_{drag} is a frictional force linearly proportional to the flow velocity \vec{v} and the drag coefficient of the trapped particle γ , which expression depends on its geometry. In the case of a cylinder of length L and radius a , moved along its longitudinal direction, the drag coefficient $\gamma_{||}$ is [6]:

$$\gamma_{||} = \frac{2\pi\eta L}{\ln\frac{L}{a} - \frac{3L}{16h} + C} \quad (9)$$

Where η is the viscosity of the suspension fluid at room temperature, h is the distance from the upper surface of the sample's micro-chamber, and $C = \ln 2 - \frac{3}{2}$ is a constant.

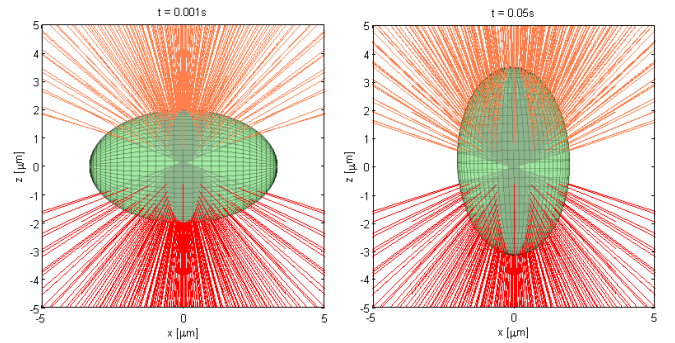


Figure 2: OTGO figure of an ellipsoid trapped with one Gaussian beam (one trap) which impinges on the particle from below. In addition to the optical force, the optical torque and the Brownian motion are computed, in order to show how the elongated particle gets aligned with the beam in a short time. Notice that there is a time indicator at the top of each figure (left: initial time, right: after 0.05 s).



Figure 3: Central part of the microscope used in the Optical Trapping Lab, evidencing the movement of the piezoelectric stage, and the location of the microscope objective lens and the condenser lens of the force measurement device.

After preparing our sample, a selection and measurement of a single cylinder was made. The width (diameter) of the particle is given by the manufacturer and is equal to $5 \mu\text{m}$. The length L is determined by counting the number of pixels N_{pix} that occupies the cylinder in the picture with an image manipulation program.

$$L = \frac{L_{pix} N_{pix}}{M} = \frac{4.65 \cdot N_{pix}}{60} \quad (10)$$

Where L_{pix} is the size of one pixel of the used detector that corresponds to $4.65 \mu\text{m}$, and M is the magnification of the microscope lens, which was 60x. An error of one pixel is contemplated which, using (10) turns into an error of $0.08 \mu\text{m}$.

Different drag forces can be applied by modifying the flow velocity \vec{v} responding to variations of the amplitude of movement A of the piezoelectric stage:

$$v = 4Af \quad (11)$$

Where f is the frequency of oscillation which was kept at 1 Hz during the whole experiment.

The position of the trapped object was measured by *Video based position detection*, that relies on tracking the particle motion by recording it, to consecutively employ centroid finding algorithms knowing the size subtended by a single pixel.

Using specific software connected to the force detection instrument, the forces exerted on the cylinder by the set of the two traps are measured. By tracking its position with the already mentioned method, the trap forces and cylinder positions can be related and studied for different separations between traps. Moreover, measurements of escape forces for seven different distances between traps were made. Escape forces correspond to those exerted by the set of traps when applying the maximum value of the drag force that keeps the particle trapped. In other words, the escape force is the maximum optical force that the traps can exert on the object and it depends on the distance between traps, as will be proven in the following section.

IV. RESULTS

The simulation was implemented using two identical Gaussian beams focused into two traps, whose forces exerted on the cylinder were computed separately, only in its longitudinal direction (perpendicular to the propagating beam). By summing these forces, the total optical force exerted by the set of traps on the cylinder is obtained, and can be plotted against a wide range of positions of the cylinder, as seen in *figure 4*, or for different distances between traps, as in *figure 5*.

All the parameters used in the laboratory describing the properties of the cylinder and the trapping beams were inputted on the simulation with no changes, excepting the power of the beams, which had to be reduced by half to match the experimental results. The need for this adjustment is probably due to the fact that aberration of the traps is not accounted for in the simulations, and therefore the simulated traps need less power than the real ones to exert the same forces on the trapped object.

First, let us evaluate the optical force exerted on a cylinder of length $34.50 \pm 0.08 \mu\text{m}$, as a function of its position from the barycenter of the two traps. Three different distances between traps, expressed as a proportion of the length of the cylinder L , were examined in order to compare the force profiles, and foresee the most advantageous scenario.

In *figure 4*, the simulation and experimental results are superposed, as well as the drag force, computed with equations (8) and (9). In the red plot labeled as $0.97L$, the set of traps are located at edges of the cylinder, situation where the optical forces exerted on it are stable and almost linear. When the traps are closer a central plateau region appears, and it gets larger as the distance between traps decreases, reaching the one-trap profile at

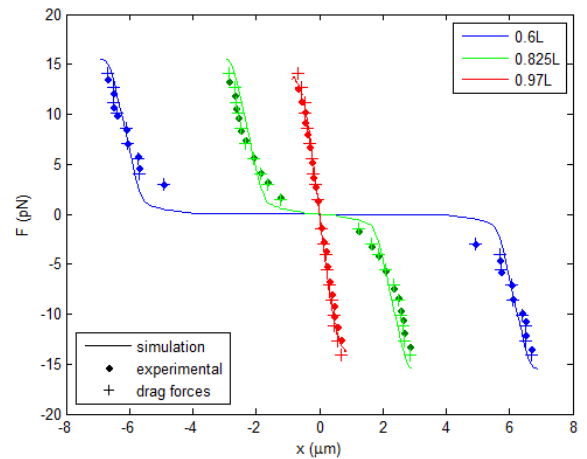


Figure 4: Forces exerted by two traps on a cylinder versus its position from the equilibrium spot, for three different distances between traps. The lines show the theoretical forces computed with OTGO, the dots correspond to experimental data and the crosses are the drag forces exerted by the suspension fluid in response to the stage movement. The error bars on the experimental data are not displayed because they are too small to be seen.

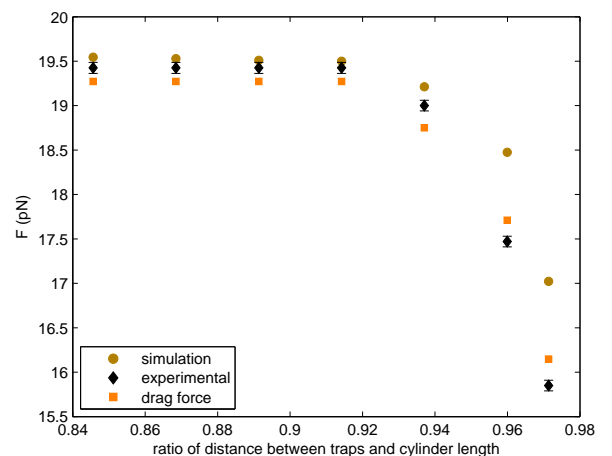


Figure 5: Escape forces exerted by the set of two traps versus the distance between them. The experimental results are shown in black, with their respective error bars. Again, the simulation results are computed with the OTGO package, and the drag forces are applied by the suspension fluid in response to the stage movement.

the limit of small distances. This behaviour shows that there is a range of positions where the set of traps are not exerting any force, and it only arises when one of them is at the edge of the cylinder, pulling it back to its equilibrium position. The computed drag forces and the experimental data are very close, and the simulation results are in very good agreement, specially when the traps are very distant.

Hereafter, the escape force as a function of the distance between traps is presented for a cylinder of length

$L = 36.43 \pm 0.08 \mu\text{m}$, superposing the simulation and experimental results and the drag forces again. They have been computed for seven different distances between traps, thus, seven points are plotted in *figure 5*. The maximum force that the set of traps can exert on the object is around $19.5 \pm 0.06 \text{ pN}$ and remains identical until the traps reach a distance of 90% the cylinder's length, where it starts to decrease. Therefore, when the distance between traps is increased above $0.9L$, the escape forces decline as the distance gets larger, hence there is a reduction of the maximum optical forces exerted on the cylinder in this range. This result was actually expected from the previous experiment (*figure 4*), where it can be observed that the red plot (corresponding to large separation between traps) shows a smaller value of maximum force compared to the other two plots representing closer traps. Even though the simulation results and drag forces are not inside the error bars of the experimental data, the maximum deviation is 1 pN, which conforms a relative error of 5%.

V. CONCLUSIONS

Although trapping complex samples could seem challenging at first, the force evaluation through directly measuring the changes in light's momentum offers a reliable and convenient approach to study unconventional settings, such as two traps holding elongated particles. In our experiments cylinders are proven to be effortlessly trapped, eliminating the need to previously attach spherical beads to be able to hold them [10][11], and therefore increasing the feasibility of the whole optical trapping technique.

The OTGO simulation package works very well on computing optical forces, and can be successfully used

to compare the obtained theoretical results with experimental measurements. However, realistic optical traps are subjected to notable aberration since high NA objectives are used, which is not contemplated in the simulation. This leads to a difference between the experimental power of the aberrated trap and the power of the ideally simulated trap, which must be reduced by half to fit in the experimental values.

Regarding both the simulation and the experimental results, it can be remarked from *figure 4* that most stable trapping happens when the traps are distant, almost at the edge of the cylinder, and decreasing the distance between traps causes that only one trap exerts force when located at one of the edges, causing a wider oscillation of the cylinder. Otherwise, the results exposed in *figure 5* reveal that when the traps are very separated, more than the 90% of the cylinder's length, the optical force exerted on it decreases, as the distance between traps increases.

Considering this, the most strong and stable way of trapping a micro-sized cylinder with a set of two optical traps occurs when the distance between them is around 0.9 times its length, and the reduction of this distance only leads to less stable trapping, but not to a decrease on the value of the optical force exerted on the cylinder.

Acknowledgments

I would like to express my gratitude to Estela Martín Badosa and Mario Montes Usategui for entrusting me with this project, and specially Estela Martín Badosa for her advice and guidance during the whole process. I am also very thankful to Frederic Català Castro for patiently teaching me all the experimental procedures, and offering a helpful hand whenever was needed.

-
- [1] A. Ashkin, J.M.Dziedzic "Optical trapping and manipulation of viruses and bacteria", *Science* **235**, 1517-1520 (1987).
 - [2] I. Verdeny, A. Farré, J. Mas, C. Lopez-Quesada, E. Martín, M. Montes-Usategui "Optical trapping: A review of essential concepts", *Optica Pura y Aplicada* **44** (3) 527-551 (2011).
 - [3] K.C. Neuman, S.M. Block "Optical trapping", *Review of scientific instruments* **75** (9) 2787-2809 (2004).
 - [4] A. Farré, E. Martín, M. Montes-Usategui "The measurement of tight momentum shines the path towards the cell", *Optica Pura y Aplicada*, **47** (3) 239-248 (2014).
 - [5] A. Farré, M. Montes-Usategui, "A force detection technique for single-beam optical traps based on direct measurement of light momentum changes," *Opt. Express* **18**, 11955-11968 (2010).
 - [6] F. Català, F. Marsà, A. Farré, M. Montes-Usategui, E. Martín "Momentum measurements with holographic optical tweezers for exploring force detection capabilities on irregular samples" *Proc. SPIE* 9164, 91640A, (2014).
 - [7] J.W. Shaevitz, "A Practical Guide to Optical Trapping", Technical report, Princeton University (2006).
 - [8] A. Callegari, M. Mijalkov, A.B. Gököz, G. Volpe "Computational toolbox for optical tweezers in geometrical optics", *Journal of the Optical Society of America*, **32**, B11-B19 (2015).
 - [9] A. Callegari, M. Mijalkov, A.B. Gököz, G. Volpe "OTGO - Optical Tweezers in Geometrical Optics, User manual and commented code examples", Technical report (2014).
 - [10] M.D. Wang, H. Yin, R. Landick, J. Gelles, S. Block *Stretching DNA with Optical Tweezers*, *Biophysical Journal*, **72** 1335-1346 (1997).
 - [11] R.M. Simmons, J.T. Finer, S. Chu, J. Spudich *Quantitative Measurements of Force and Displacement Using an Optical Trap*, *Biophysical Journal*, **70** 1813-1822 (1996).